© Universiti Tun Hussein Onn Malaysia Publisher's Office

IJIE

http://penerbit.uthm.edu.my/ojs/index.php/ijie
ISSN : 2229-838X e-ISSN : 2600-7916

The International Journal of Integrated Engineering

3D Modeling of CO_2 Geological Storage of Songkhla Sub-Basins in the Lower Gulf of Thailand

Apichat Choomkong[1], Siriphat Sirikunpitak[2], Nattaphon Temkiatvises[3], Sawasdee Yordkayhun[1*]

[1]Geophysics Research Center, Department of Physics, Faculty of Science, Prince of Songkla University, Thailand

[2]Sustainable Energy Management, Faculty of Environment Management, Prince of Songkla University, Thailand

[3]Reservoir Engineer, Schlumberger Overseas, S.A., Thailand

*Corresponding Author

DOI: https://doi.org/10.30880/ijie. 2020.12.03.006
Received 20 June 2018; Accepted 25 July 2019; Available online 28 February 2020

Abstract: Geological storage of CO_2 is one of the high efficiency CO_2 disposal methods which can help mitigate the global warming problem. The aim of this study is to construct a 3D geological model for assessing CO_2 storage capacity and direction of CO_2 migration in Songkhla basin in the Lower Gulf of Thailand. Songkhla Lower Miocene (SLM) and Songkhla Lower Oligocene (SLO) are the main target formations of CO_2 injection. 3D geological model was achieved based on integration of available depth structure map, geologic setting and reservoir properties. As the results from 3D static model, the total accumulation of CO_2 storage capacity of SLM and SLO formation is approximately 13.47 Mt (million metric tonnes). The 3D dynamic model can be used to track time lapse CO_2 plume and pressure build up in the reservoir during CO_2 injection, providing a plan for risk assessment of CO_2 leaking out of reservoir. The modeling results from this study help to demonstrate the technological feasibility of geological storage of CO_2 in Songkhla basin.

Keywords: 3D geological model, CO_2 geological storage, Songkhla Lower Miocene, Songkhla Lower Oligocene

1. Introduction

Global warming is a serious problem affecting humans and the environment, which is the most pressing challenge facing the world nowadays. The severity of these effects can be mitigated by using alternative energy and reducing dependence on fossil fuels [1]. In the past decade, Thailand has increasing demand for electricity to drive the economy. In 2014, the majority of electricity (up to 70%) came from burning fossil fuel, especially the natural gas [2]. According to the 2015 power development plan, Songkhla province, southern Thailand is possibly facing for the rising of CO_2 emissions due to electricity generation [3]. Therefore, planning to reduce greenhouse gas emissions, especially CO_2 is important to mitigate global warming follow the international agreement in COP21 [4,5]. The commitment for climate change policy is stated that Thailand has undertaken to reduce CO_2 emissions of approximately 110-140 Mt (million metric tonnes) by 2030 [4,5,6].

Even though the non-timber plants can absorb a substantial quantity of CO_2 from the atmosphere to reduce the effects of global warming [7], the extreme environmental conditions from climate change, such as water availability and soil salinity consequently become a disturbance on all phases of plant growth [8]. Recently, Carbon Capture and

*Corresponding author: sawasdee.y@psu.ac.th

Storage (CCS) technology is considered to be an effective method to reduce CO_2 emissions from large point sources and it is successfully applied in many developed countries worldwide [9,10,11]. CCS technology involves three main components; CO_2 capture, CO_2 transportation and CO_2 storage. In Thailand, Department of Mineral Fuels (DMF) under the Ministry of Energy is the responsible government agency for CCS [12,13]. A number of studies revealed that CCS project in Thailand is still in the phase of potential study. For example, assessment of CO_2 geological storage potential in a depleted oil field in the north of Thailand [14], evaluation for offshore CO_2 geological storage potential in the Gulf of Thailand [15] and a study of CO_2 emission sources and sinks in Thailand [4]. The study area for this study is Songkhla basin. Songkhla Lower Miocene (SLM) and Songkhla Lower Oligocene (SLO) reservoirs, lying deeper than 800 m and 2,000 m, below the subsurface have potential to reserve CO_2 from Chana power plant, where electricity capacity of 1500 MW/year is generated [16,17]. Moreover, this zone may support clean coal energy project with capacity approximately 2,000 MW in the near future [14]. Therefore, this study aimed at a basin-scale assessment of CO_2 storage capacity and plume development by using 3D geological model of Songkhla basin (Block G5/43) as a representative of CO_2 sink.

Previous work based on estimation of the accumulative production and proved reserved data of these blocks found that the total geological storage volume of CO_2 in SLM and SLO reservoirs is approximately 5.22 Mt/year [4]. Because of the complexity and variety of processes occurring in CO_2 storage, as well as the cost effective of geophysical and geological survey, application of reservoir simulation is extremely valuable. It is necessary for understanding the reservoir physics, field development planning, assessing uncertainly, well planning, estimation of reserves and monitoring. All available data, consisting of depth structure map, geologic setting, and reservoir properties can assist to obtain 3D geological model and decide site prospected for CO_2 geological storage.

2. CO_2 Geological Storage Site Descriptions

2.1 Geological Storage Methods

Geological storage method can keep CO_2 as a long-term from large point sources such as power generation of anthropogenic CO_2 emissions. The storage mechanisms are injecting CO_2 as a supercritical fluid and trapping in a deep of rock formation such as a saline aquifer, a depleted petroleum reservoir, a deep unmineable coal seams and etc. In CO_2 supercritical phase, defining as temperature of 31.1°C and pressure of 73.8 bar based on worldwide average geothermal and hydrostatic pressure conditions [18,19,20], the characteristic of CO_2 is much denser than CO_2 gas phase. Therefore, a greater volume of CO_2 can be stored in the porous rock within the CO_2 supercritical phase [21].

The lighter CO_2 supercritical phase will be rise upwards by buoyancy through the reservoir until trapped by differences of physical, geochemical or hydrodynamic trapping mechanisms for long times (hundreds to thousands of years). Then, the CO_2 will sink as it becomes solutions [22]. Either hydrocarbon reservoir or saline aquifer can have different trapping mechanism for different scales (1-10,000 years or even more), including structural and stratigraphy trapping, residual trapping, solubility trapping and mineral trapping [23].

2.2 Geological Setting of the Study Area

Songkhla basin is located in offshore approximately 6-11 km from Ranod district, Songkhla province with elevation below mean sea level of 18-24 m. The area covers 1,800 km^2 and has geothermal gradient of 3.8° - 4.7°c/100 m [24]. The evolution of Songkhla basin was generated in Tertiary period by tectonic influence that associated with right lateral of Mae Ping and Three Pagodas faults in N-W trending, and left lateral of Ranong and Klong Marui faults in N-NE trending. The sediment of Songkhla basin formed in Tertiary age and running in N-S trending [24,25]. The structural styles were stretched by extension and inversion [25]. The western slope of normal fault is the main structure to control the expansion and a sediment deposition. Tertiary sedimentary sequences in the west of basin is almost entirely non-marine sediments of alluvial fan domination, while lacustrine and fluvial deposited from central to the east with influenced of marine transgression [25]. The accumulation of sediment in the basin is approximately 3,500 m, classifying as a total of 5 formations. The source rock below 2,000 m are mature enough to generate hydrocarbon [24,25]. The main structures comprise faults cutting and tilted fault traps, dividing Songkhla basin in three blocks where Bua-Ban located in the southern, Benjarong located in the western and Songkhla located in the eastern of the basin [17,24,25].

Bua-Ban field is about 50 km north of the expected CO_2 emissions source from Chana power plant (CP) as shown in Fig. 1. The field consists of SLM and SLO formation, covering approximately 280 km^2 with total depth of about

2,800 m [17]. In SLM and SLO block, a number of appraisal wells and development wells were drilled in 2005 and 2010, respectively [17]. The geological setting and geographical location of SLM and SLO formations act as impact factors and boundary condition of 3D geological model for CO_2 storage in Songkhla basin.

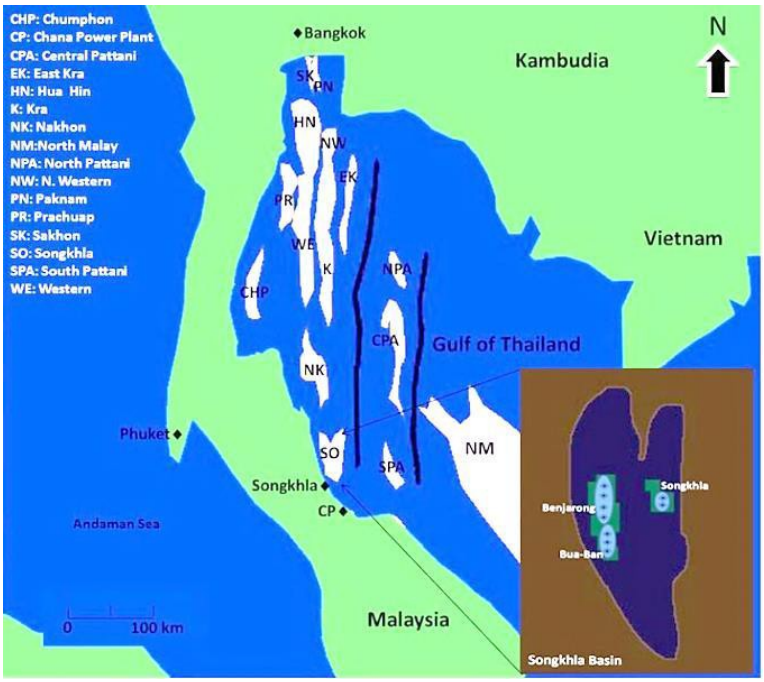

Fig. 1 - Location of CO_2 source (Chana Power Plant; CP) and CO_2 sink (Songkhla basin; SO)

3. Theoretical Background of 3D Geological Model

3.1 3D Geological Model

A static model is 3D geological representation of the reservoir and it can describe CO_2 distribution by a computational domain. A reliable 3D geological model is set up and parameterized based on geology setting and geophysical data. CO_2 migration is controlled by rock and fluid properties [26]. In particular, CO_2 storage site characteristics are associated with porosity and permeability of the reservoir. Geological models utilize discrete fracture networks (DFNs) that describe behavior of natural fracture networks in a rock formation with modeling of geo-metrical, geo-mechanical and hydro-mechanical characteristics. DFNs used a class of dual-continuum principle which the porous medium of a rock formation is represented as lines or planes in 2D or 3D model [27,28]. Dual-continuum models are based on an idealized flow medium consisting of a primary porosity created by deposition and lithification. A secondary porosity created by fracturing, jointing, or dissolution which fluid can flow in porous media of rock fracture in the reservoir. In addition, 3D static modeling used principle of elastic deformation with tensors of each physical property is derived by fracture in the rock formation [29,30,31].

3.2 Fluid Flow of Dynamic Model

After CO_2 injection, the behaviors of CO_2 movement in the rock formation depend on fluid interaction, porous media, reservoir pressure and pressure of injection well. The concept of fluid flow can comprehend the relationship between steady-state, pseudo steady-state and unsteady-state fluid flow [31]. Darcy's law and material balance equations are the main concepts to describe practical fluid flow in the reservoir. Fluid flow can be a single phase or multiple phase and is classified according to the geometric configuration, the compressibility of the fluids, and the constancy of flow rates and pressure with time [32,33].

3.2.1 The Darcy's Equation

Darcy's law is an empirical relationship derived for the vertical flow of fluid through packed sand. This equation can describe the apparent velocity (v) of a fluid flowing through a porous media as proportional to the pressure (P) gradient as illustrated in equation 1.

$$dv = - (k)\frac{1}{u}\frac{dP}{dx} \quad (1)$$

Where μ is viscosity or friction to flow and k is a constant of permeability [34]. The negative sign is added to make the velocity (dv) positive because if dx is measured in the direction of flow, the pressure (dP) will decline as dx increases. This decline results in a negative value for (dP/dx). In the volumetric, dv can be replaced with dq/dA [33], as shown in equation 2.

$$dq = -k\frac{dA}{u}\frac{dP}{dx} \quad (2)$$

Where dq is volume per time in cc/sec. dA is gross cross-sectional area in sq/cm. dP/dx is pressure gradient in atm/cm and u is viscosity in centipoise (cP); (1 cP=1 mPa*s). This equation can be adapted to oil or gas field as shown in equation 3.

$$q = - \frac{1.127kA}{u}\frac{dP}{dx} \quad (3)$$

Where k is permeability which is important parameter relate to cumulative thickness of core rock sample. The Darcy's equation can be used to explain CO_2 migration in the 3D geological model. For numerical simulation, the flow domain must be discretized in space.

3.2.2 Material balance equations

Material balance equation is based on a simple mass balances of fluids in the rock formation which formulated by principle of material conservation. That is the final amount of fluids remaining in the reservoir is equal to the amount of fluids originally present in the reservoir minus the amount of fluids produced from the reservoir [35]. In a closed reservoir, material balance equation can be described by equation 4.

$$GB_{g1} = (G - G_p)*B_{g2} \quad (4)$$

Where G is gas initially in place. G_p is cumulative gas production, and B_g is the formation volume factor for gas. This equation describes the amount of material remaining in the SLM and SLO reservoir after a production based on assumptions of rock and fluid properties do not change in space.

4. Materials and Methods

Petrel and Eclipse Ver. 2017 software (supported by Schlumberger Oversea S.A., Thailand) were used for constructing a static and dynamic mode of SLM and SLO blocks. 3D static models were constructed based on extensive investigation of existing initial conditions and reservoir properties. A depth structure map, representing the elevation of reservoir beneath the surface, faults, folds, boundary, and location of wells are displayed in Fig. 2. The elevation displayed in the depth structural map is controlled by available 164 well logs marked as red dot in Fig. 2. A width and displacement of faults have effect to surface plane of the reservoir. Thus, fault model, showing orientation and dip was created by digitizing on depth structural map using stick fault module (Fig. 3). The boundary conditions chosen for surface and base of reservoir were constructed from gamma ray log of 164 wells and seismic section based on marker correlation for horizon 1 (top formation) and horizon 2 (base formation).

The published reservoir properties data revealed that this zone has average thickness of approximately 200 m for SLM formation [17]. To generate 3D static model, average porosity of 12% and permeability of 55 mD picked from the published reservoir properties [17] are the main input parameters. Before creating a dynamic model, initial pressure and temperature, oil water contact (OWC) and fault transitional multiplier are parameters that affect the migration of injected CO_2. Gamma ray log provided lithology correlation and displayed a depth of oil water contact in the formation. The value of fault transitional multiplier can be varied from 0-100%. 0% of fault transitional multiplier means the fluid cannot flow through the fault with sealed. Whereas 100% means the fluid can completely flow through the fault. The final step is running the dynamic model by Eclipse simulator. In this step, well completion must be defined by testing of injection scenarios. Table 1 gives a summary of the main input parameters to run the 3D geological modeling.

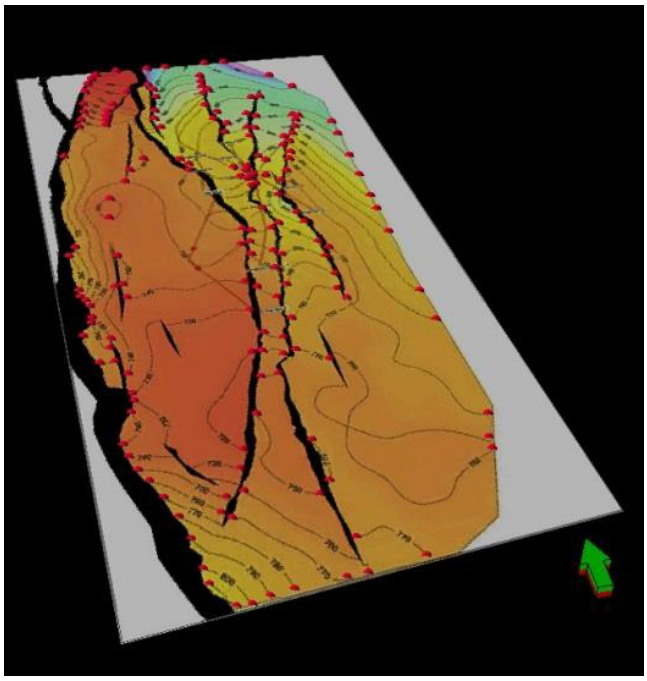

Fig. 2 - A depth structure map of SLM block, modify from [14]

5. Results and Discussions

5.1 Songkhla Lower Miocene (SLM)

3D geological model of SLM block consist of 45,451 grid cells with average grid size of X=30 m, Y=30 m and Z=200 m, corresponding to the total pore volume of 3.71×10^{10} m^3. The grid size indicated that the spatial resolution of the model is about 30 m, whereas the lack of stratigraphic heterogeneity information, limits the ability to construct a detailed reservoir model and vertical resolution. Therefore, the model reliability is verified in the qualitative manner by observing the correlation of modeled porosity and derived porosity from available gamma ray log. The acceptable agreement between those porosity values has built our confidence that the model would improves understanding of plume development, and reservoir structure, although very subtle shale layers were not taken into account. In this study, porosity distribution in the 3D static model is in the range of 2% - 24%. The most of area is occupied by porosity in the range of 12% - 14%, representing by blue zone in the 3D geological model (Fig. 4).

Table 1 - Reservoir properties of SLM and SLO formations

Reservoir properties	SLM formation	SLO formation
Top formation	734 m	1,950 m
Base formation	934 m	2,150 m
Average thickness	200 m	200 m
Porosity	12-14 %	27.5-30 %
Permeability	55 mD	55 mD
Initial pressure	230 bar	224 bar
Type of rock	Sandstone	Sandstone

To simulate the reservoir response, the existing well (Well E) locating in the high porosity zone was selected for CO_2 injection in the 3D static model. After injection, the migration of CO_2 plume around the injection well is outlined in the 3D dynamic model (Fig.5). It can be seen that the CO_2 tend to accumulates in the high porosity regions. The lateral extent of CO_2 plume, as imaged by the dynamic model is about 800 to 1000 m, with dominating westward propagation of the injected CO_2 from the injection well. In the simulation scenario, the daily injection rate of CO_2 is equal to the realistic daily CO_2 emission in a period of 1 Jan 2014 to 30 April 2015 of Chana power plant. The formation pressure limit has been set to not exceed the initial pressure of reservoir (230 bars for SLM formation) to avoid the risk of induced fracturing and fault activation in the reservoir. The result show that formation pressure

continuously increased from initial conditions to the initial pressure of 230 bars in a period of 6 months (Fig.6). The volume of CO_2 in the SLM storage formation increases almost linearly during the injection period to a maximum cumulative amount of about $9.6x10^8$ m^3. Note that the pressure drop in some periods is due to the decreasing of CO_2 emission rate from the power plant.

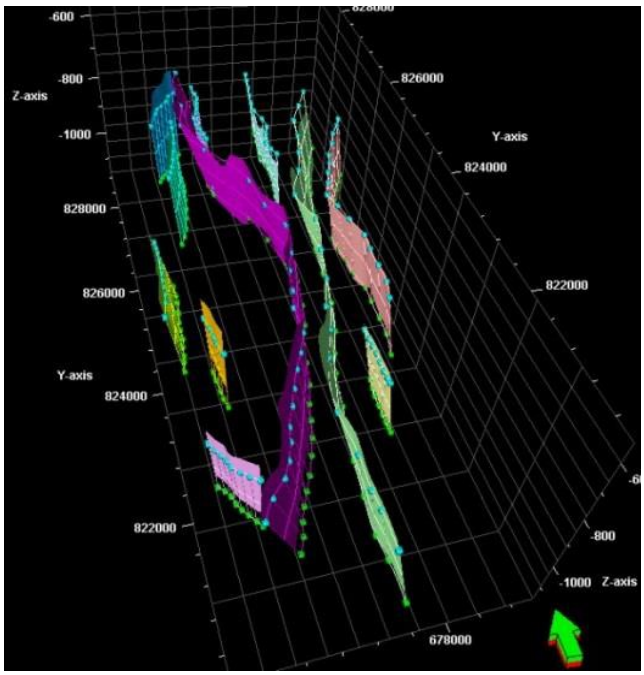

Fig. 3 - Fault model extracted from fault sticks

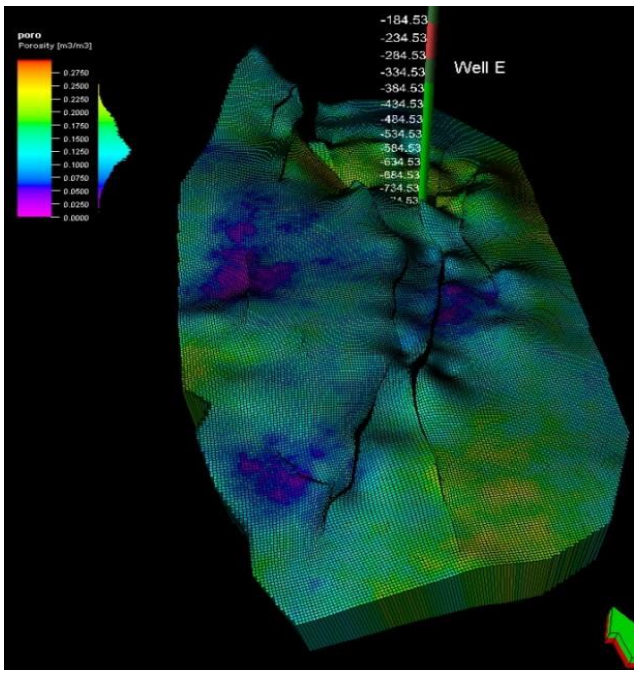

Fig. 4 - 3D geological model of SLM block showing distributions of porosity

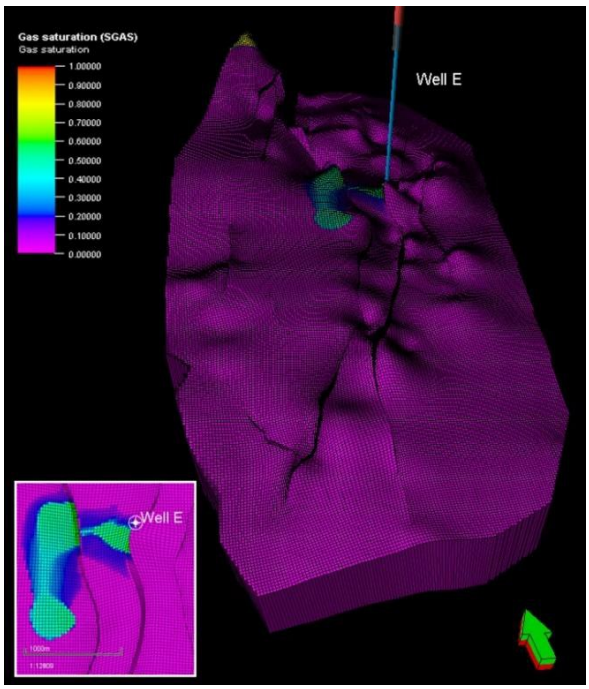

Fig. 5 - CO_2 migration in SLM block showing flow direction in the west of injection well E

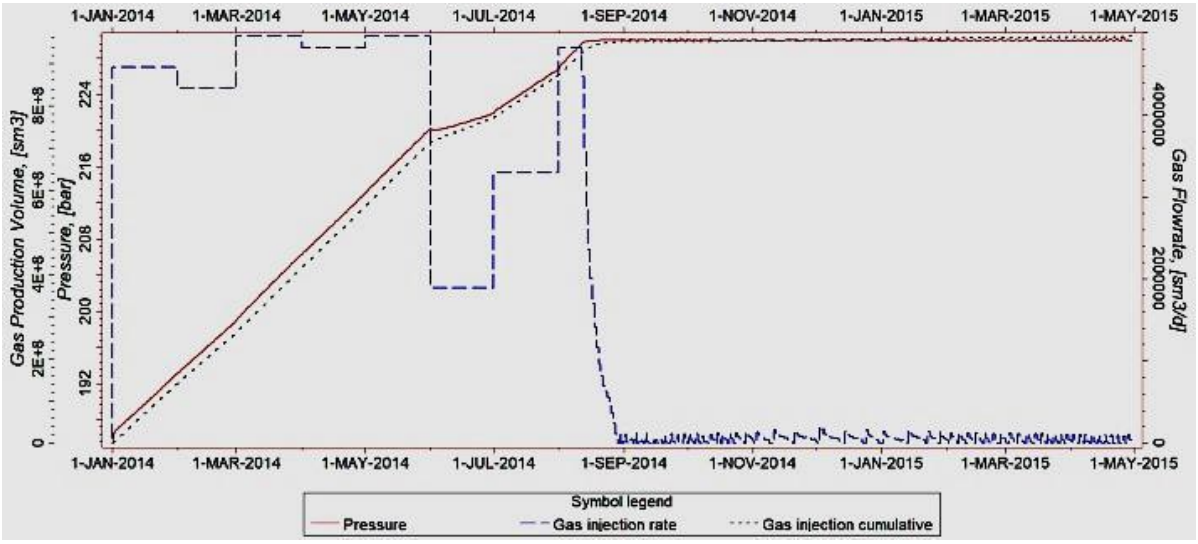

Fig. 6 - The relationship between CO_2 injection rate (stippled blue line), pressure (solid red line) and an accumulation of CO_2 (dotted black line) in the SLM block

5.2 Songkhla Lower Oligocene (SLO)

3D geological model of SLO block consist of 27,692 grid cells with average grid size of X=29.3 m, Y=30 m and Z=199.5 m, corresponding to the actual formation volume of 1.93×10^{10} m^3. As mentioned before, the detailed stratigraphy is not clearly resolved on the models, their geometry, distribution, and continuity form a large uncertainty in reservoir modelling. Porosity distribution in the 3D static model is in the range of 7.5% - 42.5%. It is observed throughout the large area of reservoir and characterized by porosity in the range of 27.5% - 30%, representing by blue-green zone in the 3D geological model (Fig. 7).

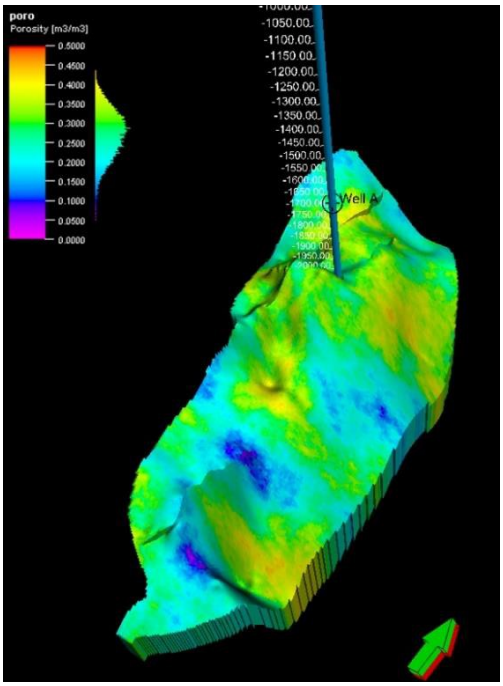

Fig. 7 - 3D Geological Model of SLO Block Showing Distributions of Porosity

The CO_2 injection well (Well A) was selected in the high porosity zone in the 3D static model of SLM formation. After injection, the migration of CO_2 plume around the injection well is demonstrated in the 3D dynamic model (Fig.8). It can be noted that the lateral extent of the CO_2 plume, is about 800 to 1000 m, in the west and about 200 m in the east of the injection well. In this simulation scenario, the injection starts after the ending of CO_2 injection in the SLM

formation. Hence, CO_2 production data from Chana power plant during 01 September 2014 - 01 August 2017 were used for the daily injection rate of CO_2. The formation pressure limit in the SLO block is controlled to not exceed the initial pressure of 224 bars. As shown in Fig.9, the cumulative amount of CO_2 injected into the SLO storage formation is about 3.81×10^9 m^3 within the period of 30 months. It is important to note that a single injection well will not be able to accommodate CO_2 for long-term period, so an increase in the number of wells must be considered for constraining the formation pressure and storage volume.

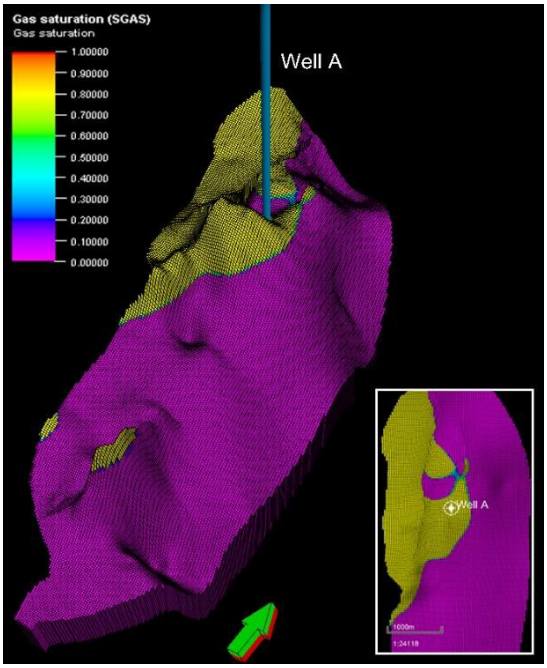

Fig. 8 - CO_2 migration in SLO block showing flow direction in the west of injection well A

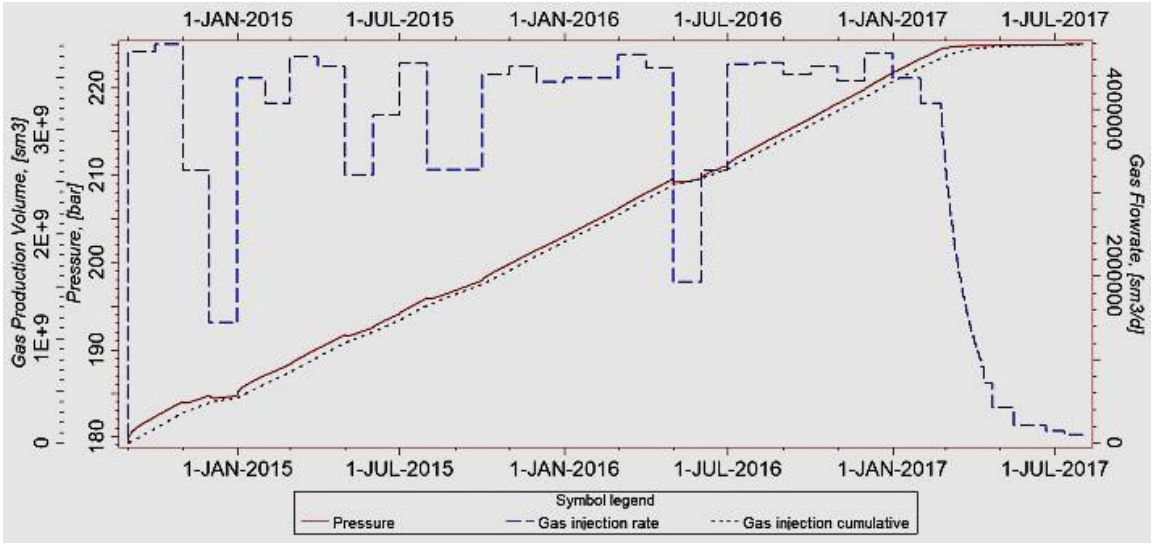

Fig. 9 - The relationship between CO_2 injection rate (stippled blue line), pressure (solid red line) and accumulation of CO_2 (dotted black line) in the SLO block

In term of storage capacity, the cumulative amount of CO_2 in gas STP volume is converted to equivalent mass of CO_2 tonnage stored using conversion equation 5 [3].

$$1\ Tcf\ (Trillion\ standard\ cubic\ feet) \approx 80\ Mt \quad (5)$$

The results highlight that CO_2 capacity and behavior are site specific. The existing two hydrocarbon fields in the Songkhla sub-basins have potential to store CO_2 up to approximately 13.47 Mt. In this case, 2.71 Mt (2.6% of total

volume) and 10.76 Mt (19.6% of total volume) of CO_2 can be injected in the SLM and SLO formation, respectively. It is clear that the assessment of effective storage capacity in the reservoir requires detailed of reservoir structure and stratigraphy. In particular, different of porosity and fault geometry play a vital role in accumulation of CO_2 storage. The migration of the injected CO_2 shows an inhomogeneous pattern, indicating that the lateral heterogeneity of the storage formation strongly affects the plume geometry. CO_2 migration simulation shows the general westward transport with plume alignment along a north-south trending, reflecting the structural trapping mechanism in the injection stage.

6. Conclusions

We have demonstrated that geological storage of CO_2 in Songkhla sub-basins has potential to be the effective method in reducing CO_2 from Chana power plant emission source. The different of fault structures and seal conditions as well as reservoir properties of SLM and SLO formation affect CO_2 capacity and plume geometry. In the injection scenario, it was demonstrated that 2.71 and 10.76 Mt-CO_2 can be injected in the SLM and SLO formation for a period of 3 years. Pathway of CO_2 movement in the reservoir can be tracked from the 3D geological model. Although the models showed promising results, there are still open questions regarding the suitable position of injection and observation wells, optimum injection rate and monitoring framework of the storage formation. Furthermore, the degree of uncertainty associated with reservoir complex is still considerable challenge of CO_2 geological storage modeling. Therefore, further tests should contribute to these aspects and might involve extending the various scenarios.

Acknowledgements

The authors would like to extend their appreciation to Schlumberger Overseas, S.A., Thailand, for supporting Petrel and Eclipse modeling software. Financial support for this work is provided by the National Research Council of Thailand (NRCT) under contract No. 555856 and Graduate School of Prince of Songkla University.

References

[1] Nda, M., Adnan, M. S., Ahmad, K. A., Usman, N., Mohammad Razi, M. A., & Daud, Z. (2018). A Review on the Causes, Effects and Mitigation of Climate Changes on the Environmental Aspects. International Journal of Integrated Engineering, 10(4).
[2] Department of Alternative Energy Development and Efficiency. (2014). Energy in Thailand facts & Figures Q1. Bangkok, Thailand: Alternative Energy and Efficiency Information Center Department of Alternative Energy Development and Efficiency Ministry of Energy.
[3] Chaiyapa, W., Esteban, M., & Kameyama, Y. (2018). Why go green Discourse analysis of motivations for Thailand's oil and gas companies to invest in renewable energy. Energy Policy, 448-459.
[4] Choomkong, A., Sirikunpitak, S., Darnsawasdi, D., & Yordkayhun, S. .(2017) A study of CO_2 Emission Sources and Sinks in Thailand. Energy Procedia, 452-457.
[5] Statement by H.E. General Prayut Chan-o-cha. (2015). Thailand's Intended Nationally Determined Contribution. General Debate of the United Nations General Assembly New York, 29 September 2015.
[6] Electricity Generating Authority of Thailand. (2016). Thailand's Intended Nationally Determined Contribution.
[7] Audu, Y., & Linatoc, A. C. (2019). Inventory and Assessment of Carbon Storage Capacity of species of Palms in Universiti Tun Husein Onn Malaysia, Main Campus, Batu Pahat, Johor Malaysia. International Journal of Integrated Engineering, 10(9).
[8] Jamil, N., Mohd Zairi, M. N., Mohd Nasim, N. A., & Pa'ee, F. (2018). Influences of Environmental Conditions to Phytoconstituents in Clitoria ternatea (Butterfly Pea Flower) - A Review. Journal of Science and Technology, 10(2).
[9] Intergovernmental Panel on Climate Change (IPCC). (2005). IPCC Special Report on Carbon Dioxide Capture and Storage. Cambridge University Press Cambridge, New York, Melbourne, Madrid, Cape Town, Singapore, Sào Paulo. 1-443.
[10] Global CCS Institute. (2015). The global status of CCS 2015: summary report - global-status-ccs-2015.
[11] Global CCS Institute. (2016). The global status of CCS 2016: summary report - global-status-ccs-2016.
[12] Witsarut, T., Trin, I., Siree, N., & Anuchit L. (2012) Carbon Capture and Storage, CCS, Study in Thailand: Result and Way Forward. September 12, 2012.
[13] Prapawit, W. (2016). CCS-M S6: Workshop on CO_2 geological storage and CO_2 for EOR." Hanoi,Vietnam, 7 June 2016.
[14] Maneeintr, K., Ruanman, N., & Juntarasakul, O. (2017). Assessment of CO_2 Geological Storage Potential in a Depleted Oil Field in the North of Thailand. Energy Procedia, 175-179.

[15] Maneeintr, K., Rawangphai, M., & Sasaki, K. (2017). Evaluation for Offshore Carbon Dioxide Geological Storage Potential in the Gulf of Thailand. Energy Procedia, 3486-3491.
[16] Energy Policy and Planning Office. (2015). Thailand Power Development Plan 2015-2036 (PDP2015).
[17] RPS. (2012). Technical update of remaining recoverable hydrocarbons for the Songkhla C field. report, Singaport: RPS Energy Limited (Singapore Branch).
[18] Intenational Energy Agency. (2013). Technology Roadmap Carbon Capture and Storage. report, France: Intenational Energy Agency.
[19] Holloway, S., & Savage, D. (1993). The potential for aquifer disposal of carbon dioxide in the UK. Energy Conversion and Management, 34, 925-932.
[20] Underschultz, J., Dance, T., Langford, R., Dodds, K., & Gente, D. (2009). Regional study on potential CO_2 geosequestration in the Collie Basin and the Southern Perth Basin of Western Australia. Volume 26, Issue 7, August 2009, Pages 1255-1273.
[21] Ennis-King, J., & Paterson, L. (2007). Coupling of geochemical reactions and convective mixing in the long-term geological storage of carbon dioxide. International Journal of Greenhouse Gas Control, 1(1), 86-93.
[22] Bachu, S., Bonijoly, D., Bradshaw, J., Burruss, R., Holloway, S., Christensen, N.P., & Mathiassen, O.M. (2007). CO_2 storage capacity estimation: Methodology and gaps. International journal of greenhouse gas control, 430-443.
[23] Zhao, B., MacMinn, C.W., & Juanes, R. (2014). "Residual trapping, solubility trapping and capillary pinning complement each other to limit CO [subscript 2] migration in deep saline aquifers." Energy Procedia (Elsevier), 3833-3839.
[24] Ridd, M. F, Barber, A. J, & Crow, M. J. (2011). The geology of Thailand. Publish by the geology social London 2011.
[25] Kaewkor, C., Watkinson, I., & Burgess, P. (2015). Structural Style and Evolution of the Songkhla Basin, western Gulf of Thailand. GEOINDO, 2015.
[26] Zhao, B., MacMinn C.W., & Juanes, R. (2014) Residual trapping, solubility trapping and capillary pinning complement each other to limit CO [subscript 2] migration in deep saline aquifers. Energy Procedia (Elsevier), 2014: 3833-3839.
[27] Negash, B.M.(2018) Field development plan Petrel basic training. power point, Schlumberger, https://www.scribd.com/document/362080284/Petrel-Basic-Training-for-Fdp
[28] Lei, Q., Latham., J.P., & Tsang, C.F. (2017). The use of discrete fracture networks for modelling coupled geomechanical and hydrological behaviour of fractured rocks. Computers and Geotechnics, 151-176.
[29] Lim, K.T., & Aziz, K. (1995). Matrix-fracture transfer shape factors for dual-porosity simulators. Petroleum Science and Engineering, 169-178.
[30] Barenblatt, G.I., Zheltov, I.P. & Kochina, I.N. (1960). Basic concepts in the theory of seepage of homogeneous liquids in fissured rocks. Prikladnaya Matematikai Mekhanika, Akad. Nauk, SSSR, 24(5), 852-864.
[31] Warren, J.E., & Root, P.J.(1963) .The Bahavior of Naturally Fractured Reservoirs. Society of Petroleum Engineers, 245-255.
[32] Stephan, S.K., & Belayneh, M. (2004). Fluid flow partitioning between fractures and a permeable rock matrix. Geophysical research letters, 1-5.
[33] Sudipta, S., Toksöz, M.N., & Burns, D.R. (2002). Fluid Flow Simulation in Fractured Reservoirs. Massachusetts Institute of Technology. Earth Resources Laboratory.
[34] Slider, H.C. (1993). Worldwide practical petroleum reservoir engineering methods. book, Oklahoma: PennWell Publishing Company.
[35] Kleppe, J. (2003). Reservoir Recovery Techniques. report, Department of Petroleum Engineering and Applied Geophysics Norwegian University of Science and Technology.